Supporting Information for Carbon-coated Si Nanoparticles Anchored on Three-dimensional Carbon Nanotube Matrix for High-Energy Stable Lithium Ion Batteries

Hua Fang[1,2,3,*], Qingsong Liu[1], Xiaohua Feng[1], Ji yan[1], Lixia Wang[1,2,3], Linghao He[1,*], Linsen Zhang [1,2,3,*], and Guoqing Wang[1,*]

1 College of Material and Chemical Engineering, Zhengzhou University of Light Industry, Zhengzhou 450001, China;

2 Ceramic Materials Research Center, Zhengzhou University of Light Industry, Zhengzhou, 450001, China;

3 Zhengzhou Key Laboratory of Green Batteries, Zhengzhou, 450001, China

* Correspondence: fh@zzuli.edu.cn (H. Fang), helinghao@zzuli.edu.cn (L. He), hnlinsenzhang@163.com (L. Zhang), gqwang@zzuli.edu.cn (G. Wang)

Content

S1. Photos of the as-prepared Si@C and Si/CNT@C powder samples

S2. Morphologies of Si NPs and Si@C composite

S3. Thermogravimetric curves of Si, Si@C, and Si/CNT@C samples.

S4. Electrochemical performance of Si, Si@C and Si/CNT@C Samples

S1. Photos of the as-prepared Si/C@RF and Si/CNT@C powder samples

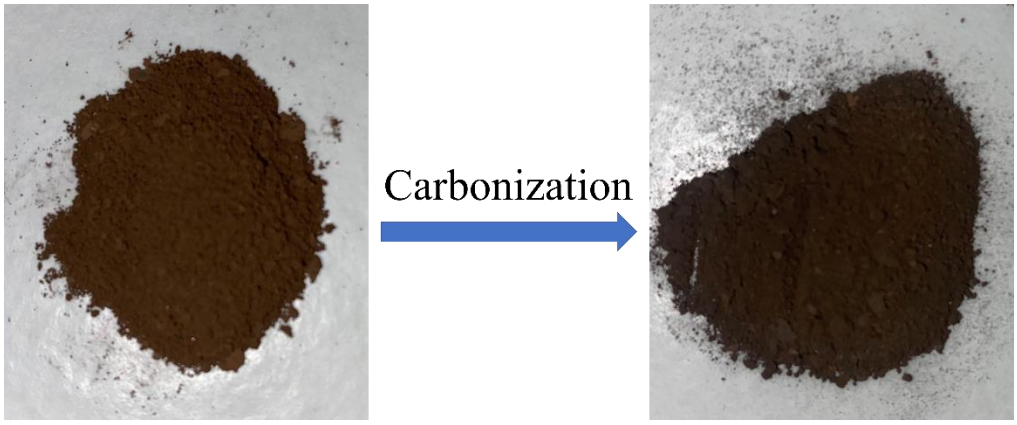

Figure S1 Photos of the as-prepared Si/C@RF and Si/CNT@C powder samples

As depicted in Figs S1, the brown power material of the Si/CNT@RF resin composite was converted to the black Si/CNT@C composite via the carbonization process. The synthesis experiment can be expanded ten times to obtain gram-grade materials, proving that the reported synthetic strategy here is highly reproducible and scalable.

S2. Morphologies of Si NPs and Si@C composite

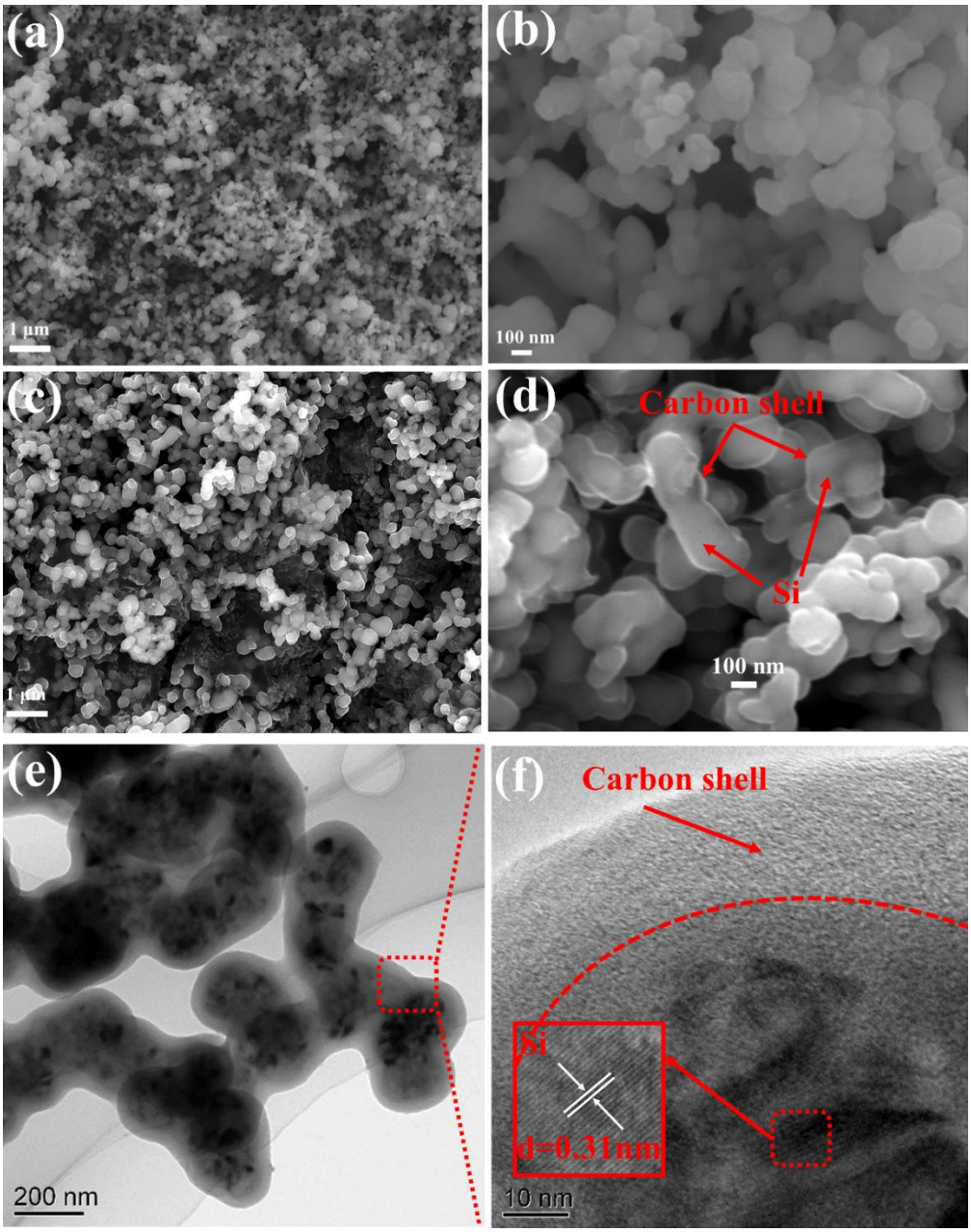

Figure S2 (a, b) SEM images of Si NPs, (c, d) SEM images, and (e, f) TEM images of Si@C composite.

As shown in Figs. S2(a, b), tiny Si NPs (50~100 nm), which were used for the fabrication of the Si/CNT@C composite, agglomerated together due to their high surface energy. After carbon coating, more obvious agglomeration can be seen from the SEM images (Figures S2c and S 2d) and TEM images (Figures S2e and S2f). The particle size of the Si@C samples reaches 100~200 nm, which conglutinated together to form much larger secondary particle aggregates. The carbon coating reaches ~10 nm thick.

S3. Thermogravimetric curves of Si, Si@C, and Si/CNT@C samples.

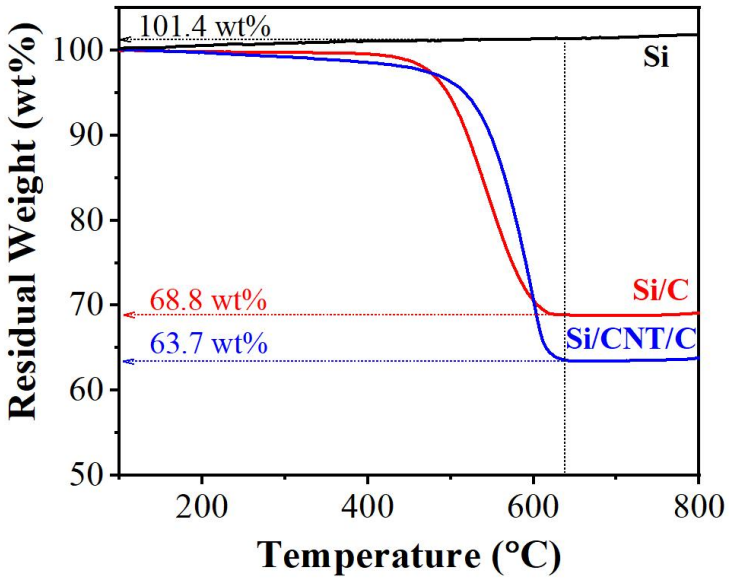

Figure S3 Thermogravimetric curves of Si, Si@C and Si/CNT@C samples

As shown in Figure S3, the weight of the bare Si NPs increased slightly (~101.4 wt%) when heat to 630 °C which can be attribute to the oxidation of silicon [1]. Taking the weight increase of bare Si into consideration, the mass ratio of Si in the Si@C sample is calculated as 68.8 wt% ÷ 101.4 wt% × 100 wt% = 67.9 wt%. Similarly, the the mass ratio of Si in the Si/CNT@C sample is calculated as 63.7 wt% ÷ 101.4 wt% × 100 wt% = 62.8 wt%. The mass ratios of carbon can be obtained by deducting the Si content from the total mass. The mass ratios of carbon in the Si@C and Si/CNT@C sample is calculated as 32.1 wt% and 37.2 wt%.

S4. Electrochemical performance of Si, Si@C and Si/CNT@C Samples

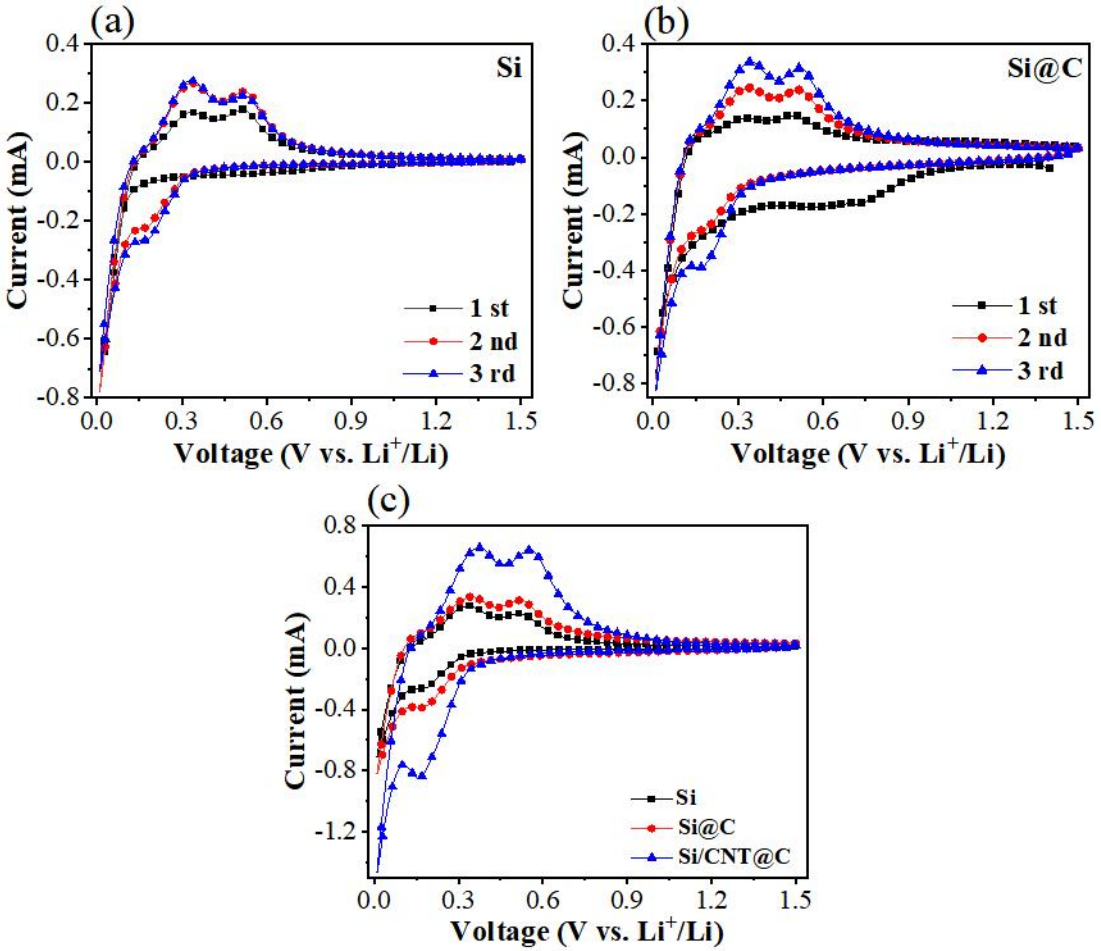

Figure S4 (a) CV curves of Si, (b) CV curves of Si@C, and (c) comparison of the third cycle CV curves of the Si, Si@C, and Si/CNT@C

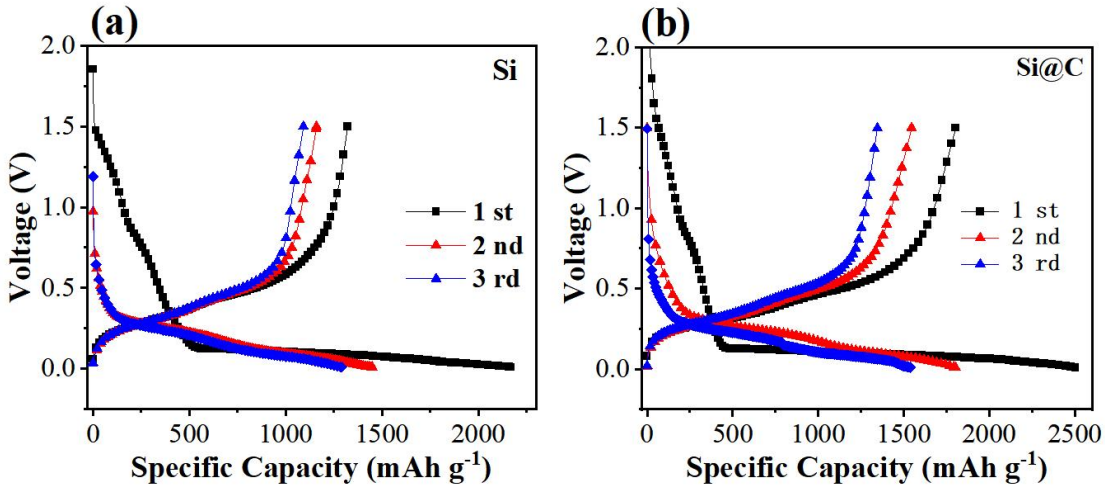

Figure S5 GCD curves of Si (a) and Si@C (b).

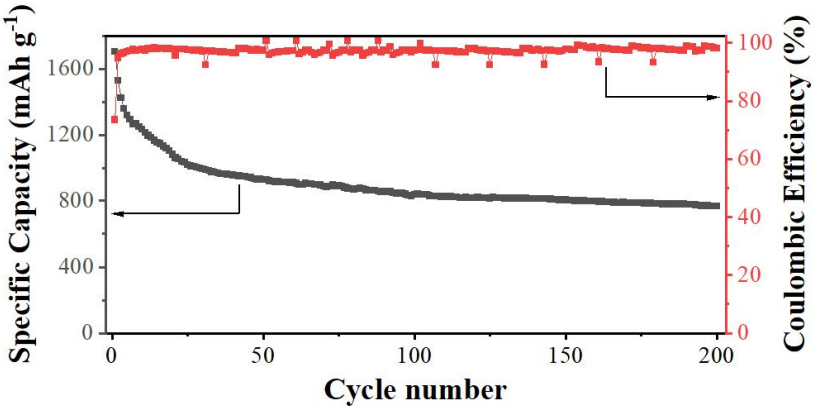

Figure S6 Cycle performances of the Si/CNT/C electrode at 0.5 A g^{-1}

Table S1 Fitting results of the EIS curves

Samples	R_s/Ω		R_{ct}/Ω		CPE				Z_W					
					CPE-T		CPE-P		W-R		W-T		W-P	
	Value	Error%	Value	Error%	Value	Error%	Value	Error%	Value	Error%	Value	Error%	Value	Error%
Si	2.0	3.06	92.5	1.70	8.2×10^{-5}	4.99	0.88	0.72	125.2	2.36	4.12	3.23	0.591	0.81
Si@C	1.7	1.61	62.4	1.03	0.00011	3.34	0.84	0.51	139.2	3.74	5.863	2.51	0.652	2.16
Si/CNT@C	1.6	3.13	38.5	1.85	7.6×10^{-5}	4.41	0.81	0.63	34.94	2.62	4.034	3.62	0.586	0.91

Note 1: CPE-T and CPE-P represent the two resistors with constant phase elements [2].

Note 2： Warburg impedance (W) represents for the solid state diffusion of Li^+ and contains three parts: ohmic resistance (W-R), diffusion time constant (W-T), and Warburg exponent (W-P) [3].

Table S2 Comparison among the recently reported Si-based anode materials

Sample	Si content (wt%)	Synthetic method	Capacity (mAh g^{-1})	Ref.
Si/CNT@C	62.8	in-situ polymerization	1106 (0.1 A g^{-1}, 200 cycles) 770 (0.5 A g^{-1}, 200 cycles)	This work
SMPS-1	12.37	Electrostatic adsorption	501 (1A g^{-1}, 500 cycles)	[4]
GSCC	39.75	self-assembly method	837.3 (0.2 A g^{-1}, 100 cycles)	[5]
Si/CNTs/C	40.4	solid-state reaction	702 (0.2 A g^{-1}, 300 cycles)	[6]
C/Si/CNTs	42.17	electrospinning	696.8 (0.1 A g^{-1}, 50 cycles)	[7]
Si@C@v@CNTs	14.1	Sol-gel + CVD	912.8 (0.1 A g^{-1}, 100 cycles)	[8]
Si/CNTs@PMMA-C	88.3	polymerization + carbonization	1024.8 (0.2 A g^{-1}, 200 cycles)	[9]
RH-Nano Si@C/CNT	72.4	electrostatic self-assembly + hydrothermal	989.5 (0.5C, 1000 cycles) (1C = 4.2 A g^{-1})	[10]
Si/CNTs@(S)-C	58.8	spray drying + template method	943 (0.2 C, 1000 cycles)	[11]

References

[1] A.-H. Liang, T.-H. Xu, S. Liou, Y.-Y. Li, Silicon Single Walled Carbon Nanotube-Embedded Pitch-Based Carbon Spheres Prepared by a Spray Process with Modified Antisolvent Precipitation for Lithium Ion Batteries, Energy & Fuels, 35 (2021) 9705-9713.

[2] J. Liang, X. Li, Z. Hou, W. Zhang, Y. Zhu, Y. Qian, A Deep Reduction and Partial Oxidation Strategy for Fabrication of Mesoporous Si Anode for Lithium Ion Batteries, ACS Nano, 10 (2016) 2295-2304.

[3] S. Saha, M. Jana, P. Khanra, P. Samanta, H. Koo, N. Chandra Murmu, T. Kuila, Band gap modified boron doped NiO/Fe3O4 nanostructure as the positive electrode for high energy asymmetric supercapacitors, RSC Advances, 6 (2016) 1380-1387.

[4] R. Xu, R. Wei, X. Hu, Y. Li, L. Wang, K. Zhang, Y. Wang, H. Zhang, F. Liang, Y. Yao, A strategy and detailed explanations to the composites of Si/MWCNTs for lithium storage, Carbon, 171 (2021) 265-275.

[5] Y. Huang, W. Li, J. Peng, Z. Wu, X. Li, X. Wang, Structure Design and Performance of the Graphite/Silicon/Carbon Nanotubes/Carbon (GSCC) Composite as the Anode of a Li-Ion Battery, Energy Fuels, 35 (2021) 13491-13498.

[6] Z. Fu, F. Bian, J. Ma, W. Zhang, Y. Gan, Y. Xia, J. Zhang, X. He, H. Huang, In Situ Synthesis of a Si/CNTs/C Composite by Directly Reacting Magnesium Silicide with Lithium Carbonate for Enhanced Lithium Storage Capability, Energy Fuels, 35 (2021) 20386-20393.

[7] X. Kong, S. Luo, L. Rong, X. Xie, S. Zhou, Z. Chen, A. Pan, Enveloping a Si/N-doped carbon composite in a CNT-reinforced fibrous network as flexible anodes for high performance lithium-ion batteries, Inorg. Chem. Front., 8 (2021) 4386-4394.

[8] N. Han, J. Li, X. Wang, C. Zhang, G. Liu, X. Li, J. Qu, Z. Peng, X. Zhu, L. Zhang, Flexible Carbon Nanotubes Confined Yolk-Shelled Silicon-Based Anode with Superior Conductivity for Lithium Storage, Nanomaterials-BASEL, 11 (2021) 699.

[9] J. Shi, X. Jiang, B. Ban, J. Li, J. Chen, Carbon nanotubes-enhanced lithium storage capacity of recovered silicon/carbon anodes produced from solar-grade silicon kerf scrap, Electrochimica Acta, 381 (2021) 138269.

[10] W. An, B. Xiang, J. Fu, S. Mei, S. Guo, K. Huo, X. Zhang, B. Gao, P.K. Chu, Three-dimensional carbon-coating silicon nanoparticles welded on carbon nanotubes composites for high-stability lithium-ion battery anodes, Appl. Surf. Sci., 479 (2019) 896-902.

[11] H. Zhang, X. Zhang, H. Jin, P. Zong, Y. Bai, K. Lian, H. Xu, F. Ma, A robust hierarchical 3D Si/CNTs composite with void and carbon shell as Li-ion battery anodes, Chem. Eng. J., 360 (2019) 974-981.